Regulation of Torsin ATPases by LAP1 and LULL1

Chenguang Zhao, Rebecca S. H. Brown, Anna R. Chase, Markus R. Eisele, and Christian Schlieker[1]

Department of Molecular Biophysics and Biochemistry, Yale University, New Haven, CT 06520-8114

Edited by Tom A. Rapoport, Harvard Medical School, Howard Hughes Medical Institute, Boston, MA, and approved March 7, 2013 (received for review January 22, 2013)

TorsinA is a membrane-associated AAA+ (ATPases associated with a variety of cellular activities) ATPase implicated in primary dystonia, an autosomal-dominant movement disorder. We reconstituted TorsinA and its cofactors in vitro and show that TorsinA does not display ATPase activity in isolation; ATP hydrolysis is induced upon association with LAP1 and LULL1, type II transmembrane proteins residing in the nuclear envelope and endoplasmic reticulum. This interaction requires TorsinA to be in the ATP-bound state, and can be attributed to the luminal domains of LAP1 and LULL1. This ATPase activator function controls the activities of other members of the Torsin family in distinct fashion, leading to an acceleration of the hydrolysis step by up to two orders of magnitude. The dystonia-causing mutant of TorsinA is defective in this activation mechanism, suggesting a loss-of-function mechanism for this congenital disorder.

DYT1 dystonia | LINC complex | nuclear egress

Early-onset DYT1 dystonia is a severe movement disorder that is caused by an in-frame GAG deletion in the *TOR1A* gene (1). This lesion results in the loss of one of two consecutive glutamate residues (E302 and E303) in TorsinA (TorA), a member of the AAA+ (ATPases associated with a variety of cellular activities) ATPases (2). Members of this superfamily typically assemble into ring-shaped, often hexameric, assemblies and use the energy of ATP hydrolysis to exert force on their substrates. In many cases, this force is invested in unfolding of targeted polypeptides or disassembly of protein complexes (3).

Of the four torsins that are encoded in the human genome (TorsinA, TorsinB, Torsin2A, Torsin3A), TorA is by far the best characterized (for a recent review, see ref. 4). TorA is broadly expressed in humans (1), and is more abundant in neuronal than in nonneuronal tissues in mice (5). TorsinA-null mice exhibit early postnatal lethality despite a lack of obvious developmental defects (6). Neurons in the CNS of these mice display abnormalities of the nuclear envelope (NE), namely a build-up of vesicular structures in the perinuclear space. A highly similar phenotype was seen in "knock-in" *Tor1A*$^{\Delta gag/\Delta gag}$ mice where the GAG deletion in the Tor1A gene was introduced into the TorA-null background. That the dystonia-associated TorA allele fails to rescue the phenotype of a TorA-deficient mouse model thus suggests a loss-of-function mechanism (6).

What is known about the molecular properties and function of TorA? TorA features an N-terminal signal sequence that directs it into the lumen of the endoplasmic reticulum (ER), where the signal sequence is removed and two *N*-glycans are installed (7, 8). TorA is recruited to the luminal side of the membrane by virtue of an N-terminal hydrophobic domain (Fig. S1*A*) (9, 10), which additionally serves to exclude TorA from ER exit sites (11). WT TorA is partitioned between the ER and NE, whereas the dystonia-associated mutant (hereafter referred to as TorA ΔE) forms inclusions in the NE (6, 7, 12–14). TorA "trap" mutants rendered ATP hydrolysis-deficient by mutating a residue in the Walker B motif (TorA E171Q) are concentrated at the NE, suggesting a function for TorA in the NE (13, 14). Two type II transmembrane proteins have been implicated in controlling the subcellular localization of TorA: lamina-associated polypeptide (LAP1) binds to the nuclear lamina in the nucleus (15), while recruiting TorA to the NE (16). Similarly, LULL1, which features a LAP1-like luminal domain (LD), associates with TorA as well (16). Whether these interactions are direct or indirect is at present unknown. Of note, a LAP1-deficient mouse model displays perinatal lethality. CNS neurons of these animals feature NE abnormalities that phenocopy those seen in *Tor1A*$^{-/-}$ or *Tor1A*$^{\Delta gag/\Delta gag}$ animals (5), suggesting that TorA and LAP1 might act in the same pathway. However, the mechanistic basis and functional significance of these interactions are currently not well understood. Indeed, a functional assignment is lacking for the majority of the proteins that have been identified as components of the NE (17, 18). At present, our mechanistic understanding of TorA in the functional context of its binding partners is hampered by the absence of a suitable in vitro system.

Here we report a functional in vitro reconstitution of TorA with its NE-resident binding partners and elucidate a role for LAP1 and LULL1 as regulatory cofactors that are responsible for the activation of TorA's dormant ATPase activity. Furthermore, we demonstrate that most but not all Torsins are regulated via a similar mechanism and thus establish a unique and conserved regulatory role for these proteins. This study extends our view of NE constituents—often perceived as passive scaffolding components—and provides a quantitative and direct demonstration of a loss-of-function mechanism in the context of primary dystonia.

Results

Glutamate Residue Deleted in Primary Dystonia Contributes to a Solvent-Exposed Acidic Patch on the Surface of TorsinA. In the absence of structural information for TorsinA, we generated a structure model comprising residues 30–327. A cartoon representation of the TorA model is given in Fig. S1. Given that the AAA domains of many experimentally determined structures are highly similar (19), we expect our model to be fairly accurate. The glutamate residues (E302/E303) affected in primary dystonia, shown as spheres, are located in the C-terminal four-helix bundle of the AAA domain. Both residues are predicted to be solvent exposed and contribute to an acidic patch (Fig. S1*C*).

Significance

Torsins belong to the AAA+ (ATPases associated with a variety of cellular activities) ATPase superfamily, the members of which disassemble protein complexes or unfold proteins. Here, we provide evidence that the activity of Torsins is tightly regulated by two proteins that reside in the endoplasmic reticulum and the perinuclear space. This regulatory mechanism provides the framework for a better understanding of phenotypes in animal models, and allows us to define the molecular defect underlying TorsinA dystonia.

Author contributions: C.Z. and C.S. designed research; C.Z., R.S.H.B., A.R.C., M.R.E., and C.S. performed research; C.Z., R.S.H.B., A.R.C., M.R.E., and C.S. contributed new reagents/analytic tools; C.Z., R.S.H.B., A.R.C., M.R.E., and C.S. analyzed data; and C.Z., R.S.H.B., A.R.C., and C.S. wrote the paper.

The authors declare no conflict of interest.

This article is a PNAS Direct Submission.

[1]To whom correspondence should be addressed. E-mail: christian.schlieker@yale.edu.

This article contains supporting information online at www.pnas.org/lookup/suppl/doi:10.1073/pnas.1300676110/-/DCSupplemental.

TorA migrates in blue native polyacrylamide gels at a position that suggests a hexameric oligomerization state (9). Thus, we generated a hexameric model to assess how the glutamate residues are positioned therein (Fig. S1 *D* and *E*). Although approximately half of the N-terminal hydrophobic domain is not represented in our model, the fact that all of the N termini are predicted to orient toward one side of the structure leads us to assume that the hexamer is oriented relative to the membrane as depicted in Fig. S1*E*, allowing for immersion of the hydrophobic domains on the upper face of the hexamer into the lipid bilayer. In this orientation, E302/E303 would be positioned on the luminal face of the hexamer, being accessible from the ER/NE lumen. Thus, TorA interaction partners that are known to reside in the ER/NE lumen are candidates to interact with TorsinA in a manner that is sensitive to structural alterations imposed by the glutamate deletion.

LAP1 and LULL1 Associate with TorsinA via Their Luminal Domains in Vivo. To determine which interactions of TorA are affected by the dystonia-causing mutation, C-terminally HA-tagged TorA expression constructs, including TorA WT, TorA ΔE (specifically, TorA ΔE302), and TorA E171Q, were cloned. The latter mutant was chosen because it is predicted to be trapped in an ATP-bound state and such ATP "trapped" mutants show a high affinity for substrate or cofactor binding in related ATPases (3). We also created a construct with both the TorA E171Q and TorA ΔE mutations, designated TorA E171Q/ΔE. HEK 293T cells were transfected with TorA WT or its mutant derivatives and metabolically labeled with ^{35}S methionine/cysteine. Mild detergent extracts were prepared from transfectants 24 h posttransfection, and subjected to immunoprecipitation with anti-HA antibodies in the presence of 2 mM ATP. The resulting immunoprecipitates were resolved by SDS/PAGE and visualized via autoradiography (Fig. 1*A*). The most prominent interaction partner, which associated with all TorA variants indiscriminately, was calnexin (Fig. 1*A*). Because this previously reported interaction (20) was insensitive to the dystonia-causing mutation, we shall address its significance elsewhere.

Notably, a protein with an apparent molecular mass of ~60 kDa was uniquely present in the immunoprecipitate derived from TorA E171Q cells (Fig. 1*A*). This observation immediately suggests that this protein binds selectively to the ATP-bound state of TorsinA. Importantly, this interaction was not seen in the additional presence of the ΔE mutation (Fig. 1*A*). Thus, this interaction partner is a prime candidate for further investigation in relation to primary

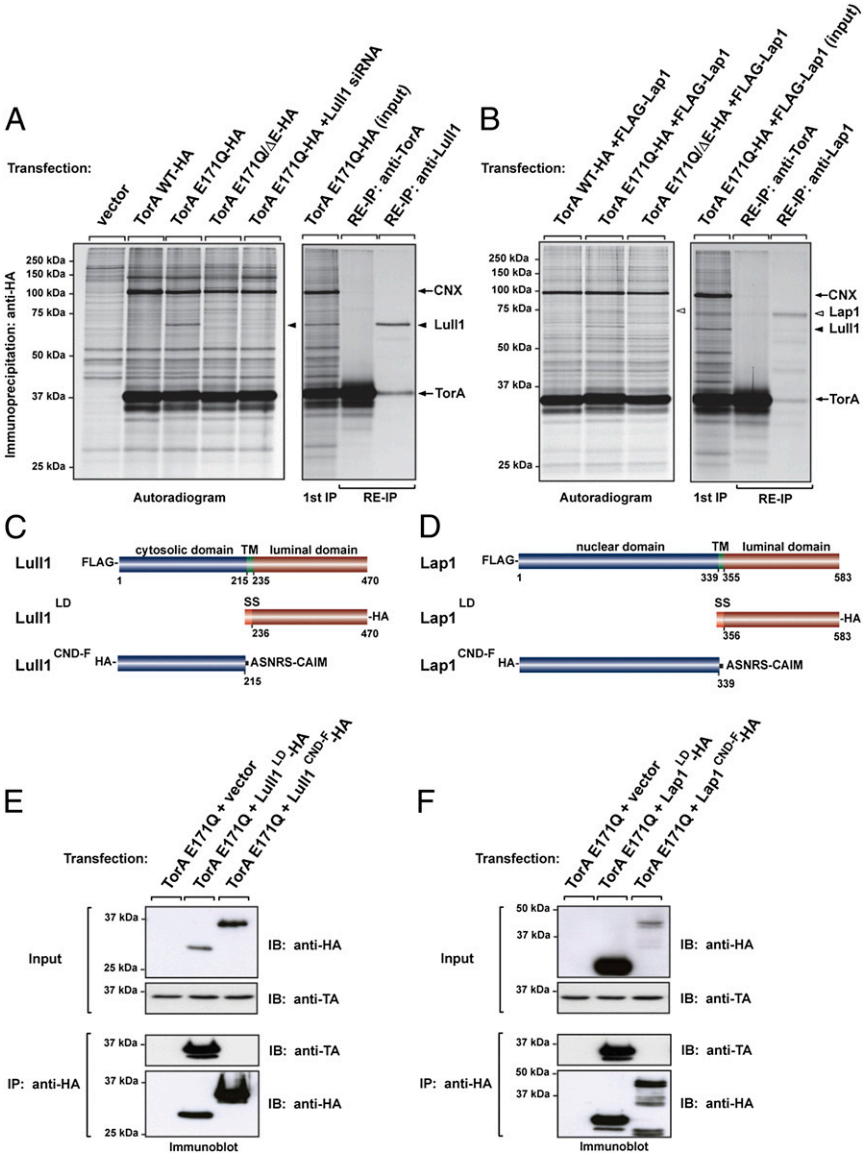

Fig. 1. The LDs of LAP1 and LULL1 are necessary and sufficient for interaction with TorsinA in vivo. (*A*) An ATP arrested TorsinA mutant associates with LULL1. (*Left*) 293T cells were transfected with the indicated constructs, metabolically labeled with 35S methionine, and lysed in mild detergent 24 h posttransfection. Following immunoprecipitation with anti-HA antibodies, eluates were resolved by SDS/PAGE and visualized by autoradiography. CNX, calnexin. (*Right*) An immunoprecipitate obtained from TorAE171Q transfectants was eluted with SDS, diluted in buffer, and reimmunoprecipitated successively using anti-LULL1 and anti-TorA antibodies. The resulting immunoprecipitates were subjected to SDS/PAGE and autoradiography. Fifty percent of the eluate used for immunoprecipitation was loaded for comparison (input, left lane). (*B*) TorA E171Q associates with LAP1. (*Left*) 293T cells were transfected with the indicated constructs and subjected to an immunoprecipitation experiment as described in *A*. (*Right*) A reimmunoprecipitation experiment was performed as described above, using an anti-HA immunoprecipitate obtained from a TorA E171Q/FLAG-LAP1 double transfectant as starting material. Anti-TorA and anti-LAP1 antisera were used for reimmunoprecipitation. (*C* and *D*) Schematic view of LULL1 (*C*) and LAP1 (*D*) constructs used in this study. TM, transmembrane domain; SS, signal sequence. (*E* and *F*) The LDs of LULL1 and LAP1 associate with TorsinA. 293T cells were transfected with the indicated constructs, and subjected to mild detergent lysis and anti-HA immunoprecipitation. Input controls and immunoprecipitates were resolved by SDS/PAGE and subjected to immunoblotting using the indicated antibodies.

dystonia. Given that the apparent molecular mass of ~60 kDa is in the range of LULL1 (theoretical molecular mass = 51.3 kDa), a known TorA interaction partner (16, 20), we repeated this experiment in cells that were pretransfected with a LULL1 siRNA pool. Under these conditions, the 60-kDa band is no longer observed, suggesting that this species is indeed LULL1. This interpretation was confirmed by dissociating an anti-HA immunoprecipitate obtained from TorA E171Q transfectants, followed by reimmunoprecipitation of the eluate using an anti-LULL1 antiserum: this antiserum selectively retrieved the 60-kDa band that we ascribed to LULL1 (Fig. 1*A*, *Right*).

We next tested if the related LAP1 protein shares the binding characteristics of LULL1. FLAG-tagged LAP1 was cotransfected with HA-tagged TorA WT and mutant derivatives, and subjected to anti-HA immunoprecipitation after metabolic labeling. Following SDS/PAGE and autoradiography, an additional band with the expected molecular mass of FLAG-LAP1 (67.3 kDa) was indeed observed that was absent from controls (Fig. 1*B*). To confirm the proposed identity of this band, we dissociated immunoprecipitates obtained from a duplicate FLAG-LAP1/TorA E171Q transfection, and subjected them to a secondary immunoprecipitation using an anti-LAP1 antiserum. The resulting autoradiogram unambiguously confirms our previous interpretation: the electrophoretic mobility of the obtained species corresponds exactly to the band ascribed to LAP1 (Fig. 1*B*, *Right*). That endogenous LAP1 was not seen in the autoradiogram we attribute to its inefficient solubilization from the nuclear lamina at the moderate salt concentrations (20) used in our experiments.

We next investigated which domains of LAP1 and LULL1 are responsible for the interaction. The most likely candidates are the LDs (see Fig. 1 *C* and *D* for domain architecture). This assumption derives support from the observation that the ectopic expression of LAP1/LULL1 constructs that encompass the LDs change the subcellular localization of TorA, but constructs that lack them do not (16). Because there is, to our knowledge, no direct evidence for a physical interaction between the LDs of LAP1 or LULL1 and TorA, we engineered expression constructs of these domains by installing a cleavable signal sequence on the N-terminal boundary of the LD, and an HA tag at the C terminus. The corresponding proteins, designated $LAP1^{LD}$ and $LULL1^{LD}$, are correctly targeted to the ER lumen, as judged by immunofluorescence microscopy (Fig. S2).

To determine whether $LAP1^{LD}$ and $LULL1^{LD}$ indeed associate with TorA, we cotransfected either construct with TorA E171Q or a vector control, prepared detergent extracts 24 h post-transfection, and subjected them to immunoprecipitation using anti-HA antibodies. Immunoprecipitates were resolved by SDS/PAGE and analyzed by immunoblotting using an anti-TorA antiserum. TorsinA was only detectable in immunoprecipitates obtained from $LAP1^{LD}$- or $LULL1^{LD}$-expressing cells (Fig. 1 *E* and *F*). To exclude the formal possibility that the N-terminal cytosolic/nuclear domains (CNDs) of LAP1 and LULL1 contribute to the interaction indirectly, we also cloned these CNDs, equipped with an N-terminal HA tag and a C-terminal farnesylation signal for membrane recruitment. As expected, an interaction between TorA and the CNDs was not observed (Fig. 1 *E* and *F*).

We conclude that LAP1 and LULL1 associate with TorsinA preferentially in its ATP-bound form in a manner that is sensitive to the dystonia-causing mutation. We additionally demonstrate that the LDs of these membrane proteins are necessary and sufficient for this interaction, which may be direct or indirect.

LAP1 and LULL1 Associate with TorsinA via Their LDs in Vitro. To unambiguously establish whether the interaction between LULL1/LAP1 and TorA is direct or indirect, we set up in vitro experiments using purified components. Because full-length TorA bears an N-terminal hydrophobic domain of established importance (Fig. S1*A*) (11), we chose to express full-length TorA and its mutant derivatives in a baculovirus system. We therefore included the mild detergent dodecylmaltoside (DDM) throughout the purification and all biochemical experiments described hereafter (*Methods*). TorA WT and its mutant derivatives were purified to ~95% homogeneity (Fig. 2*A*). The complex banding pattern of purified TorA was reduced to one band by addition of Peptide *N*-Glycanase F (PNGaseF), indicating that the apparent heterogeneity is attributable to incomplete *N*-glycosylation (Fig. 2*A*). The LDs of LAP1 and LULL1 were expressed in *Escherichia coli* and purified to apparent homogeneity (Fig. 2*A*).

We started our analysis by subjecting $LAP1^{LD}$ and $LULL1^{LD}$ to size-exclusion chromatography. Based on the UV absorption trace, both proteins eluted between the 44-kDa and 17-kDa marker proteins of a size standard used for calibration (Fig. 2*B*). This finding is consistent with a predicted molecular mass of 26.6 kDa and 27.1 kDa for $LAP1^{LD}$ and $LULL1^{LD}$, respectively. We conclude that $LAP1^{LD}$ and $LULL1^{LD}$ are monomeric under the tested conditions. We additionally confirmed the identity of the UV peaks by subjecting the corresponding elution fractions to immunoblotting, using antisera raised against $LAP1^{LD}$ and $LULL1^{LD}$ (Fig. 2*B*).

We next tested whether the elution profile of $LAP1^{LD}$ or $LULL1^{LD}$ is shifted to the high-molecular mass range in the presence of TorA E171Q, which would be indicative of a direct interaction. TorA E171Q was incubated with a twofold (monomer: monomer) excess of $LAP1^{LD}$ or $LULL1^{LD}$ in the presence of 2 mM ATP and subjected to a gel-filtration column that was preequilibrated in 500 μM ATP. A substantial shift toward the high molecular-mass range was observed both for $LAP1^{LD}$ or $LULL1^{LD}$, as judged by immunoblotting of the resulting fractions (Fig. 2 *B* and *C*). This effect was more pronounced for $LULL1^{LD}$, suggesting that LULL1 has a higher affinity for TorsinA. Correspondingly, the absorption maximum of the peak corresponding to free (monomeric) $LAP1^{LD}$ or $LULL1^{LD}$ was reduced (Fig. 2*C*).

To establish whether ATP is required for this interaction, we repeated these experiments but omitted the nucleotide both in the binding reaction and the gel-filtration buffer. Under these conditions, the shift of the elution profiles of $LAP1^{LD}$ and $LULL1^{LD}$ upon addition of TorA E171Q was greatly reduced (Fig. 2*D*). This finding was again confirmed by immunoblotting of the fractions (Fig. 2*D*). In all, these data substantiate our earlier proposal that it is in its ATP bound state that TorA has a high affinity to LAP1 or LULL1 (for additional controls, see Fig. S3).

LAP1 and LULL1 Do Not Efficiently Interact with TorA E171Q/ΔE in Vitro. We next investigated whether the dystonia-associated glutamate deletion affects LAP1 or LULL1 binding. TorA E171Q/ΔE was incubated with $LAP1^{LD}$ or $LULL1^{LD}$ in presence of 2 mM ATP and subjected to a gel-filtration column that was preequilibrated in 500 μM ATP, as described above for the TorA E171Q mutant. We did not observe a significant shift to an earlier elution volume for either LD, as judged by immunoblotting of the obtained fractions (Fig. 2*E*). We conclude that the interaction of TorA E171Q/ΔE with both LDs is significantly impaired relative to the TorA E171Q trap mutant, which binds both domains tightly. Thus, the in vitro data (Fig. 2) are in perfect agreement with our binding studies in a cellular context (Fig. 1).

LDs of LAP1 and LULL1 Induce the ATPase Activity of TorsinA. What are the functional consequences of LAP1 and LULL1 association with TorsinA? We first tested whether LAP1 or LULL1 affect the ATPase activity of TorA. Three micromolars of TorA WT was incubated in the presence of 2 mM ATP, and phosphate release was monitored at an endpoint after 60-min incubation. Surprisingly, phosphate release in the presence of TorA WT did not differ from background controls, indicating that TorsinA alone is catalytically inactive (Fig. 3*A*).

Next, TorA WT was incubated in the additional presence of 3 μM $LAP1^{LD}$ or $LULL1^{LD}$. Both proteins potently induced the

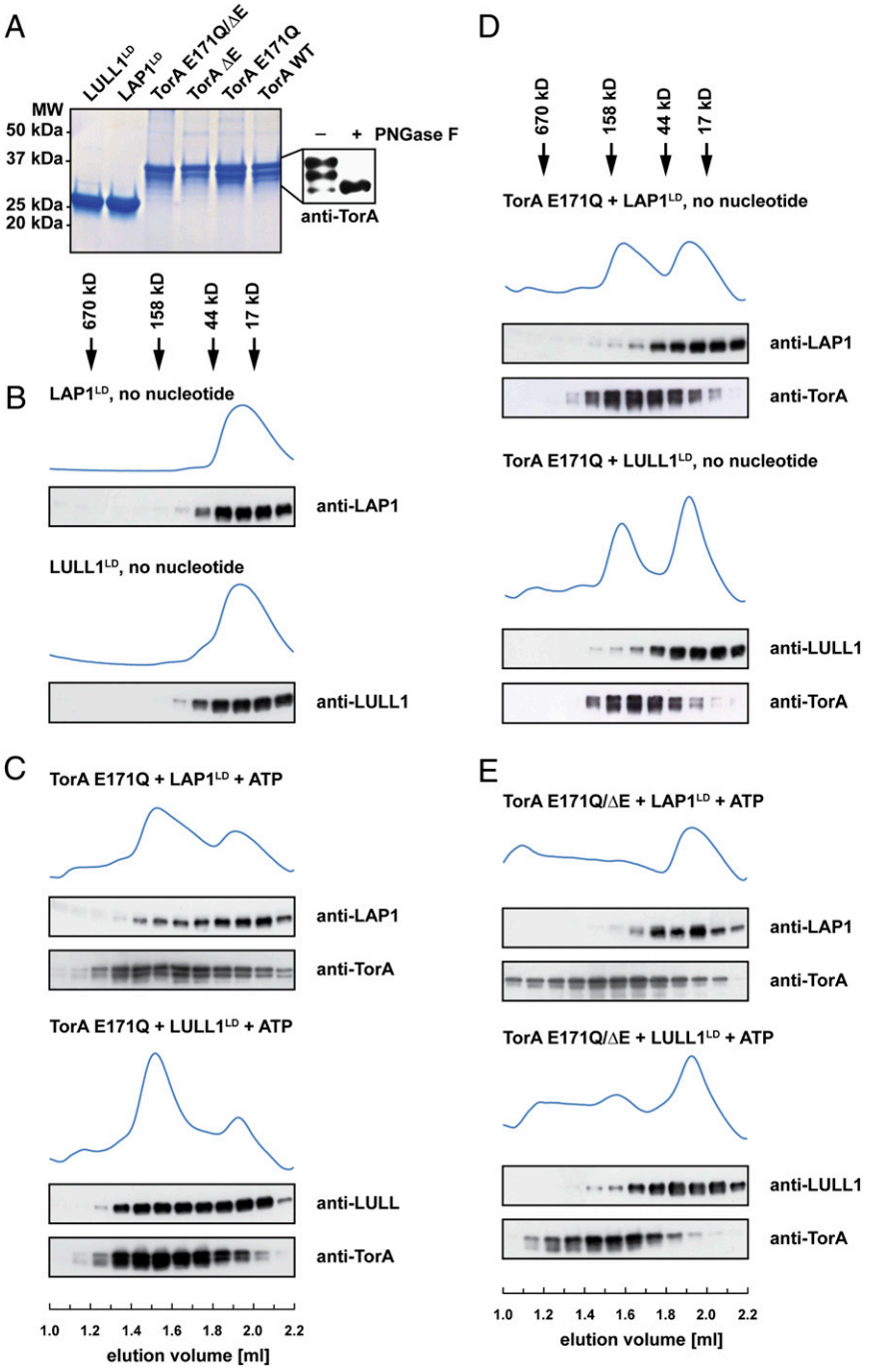

Fig. 2. The physical association of LAP1 and LULL1 with TorsinA is direct and ATP-dependent. (*A*, *Left*) Purified LDs of LAP1 and LULL1 along with TorsinA or indicated mutant derivatives were subjected to SDS/PAGE and colloidal blue staining. (*Right*) Purified TorA WT was deglycosylated by incubation with PNGase F and subjected to SDS/PAGE and immunoblotting using anti-TorsinA antibodies. (*B*–*E*) Protein complex formation was monitored by size-exclusion chromatography. UV traces are shown in blue, elution positions of size markers are indicated by arrows on top. Elution fractions were subjected to immunoblotting using the indicated antibodies. (*B*) LDs of LAP1 or LULL1 were subjected to size-exclusion chromatography. (*C*) TorA E171Q was incubated with a twofold molar excess of $LAP1^{LD}$ or $LULL1^{LD}$ in the presence of 2 mM ATP and subjected to a Superdex 200 PC 3.2/30 column preequilibrated in 500 μM ATP. (*D*) TorA E171Q was incubated with a twofold molar excess of $LAP1^{LD}$ or $LULL1^{LD}$ in the absence of ATP during incubation or chromatographic separation. (*E*) TorA E171Q/ΔE was incubated with a twofold molar excess of $LAP1^{LD}$ or $LULL1^{LD}$ in presence of 2 mM ATP and analyzed as in *B*. Note that additional controls are shown in the supplement (Fig. S3).

ATPase activity, with $LULL1^{LD}$ being more efficient than $LAP1^{LD}$ at identical concentrations (Fig. 3*A*). This observation suggests that LAP1 and LULL1 are positive regulators of TorsinA's ATPase activity.

To rule out that the observed ATPase activity is attributable to a contaminating ATPase that was inadvertently copurified, we additionally tested the TorA E171Q mutant. Analogous mutations in related AAA+ ATPases render them catalytically inactive (ref. 3 and references therein). The fact that TorA E171Q does not display ATPase activity alone or in combination with $LAP1^{LD}$ or $LULL1^{LD}$ excludes this possibility (Fig. 3*A*).

Finally, we tested TorA ΔE. TorA ΔE did not display activity in absence of $LAP1^{LD}$ or $LULL1^{LD}$, as was observed for TorA WT. More importantly, TorA ΔE activity failed to respond to addition of LAP1 and LULL1 (Fig. 3*A*). This finding therefore correlates the defect in LAP1/LULL1 binding (Figs. 1 and 2) with a lack of ATPase induction (Fig. 3*A*). It seems reasonable to propose that this molecular defect is a major contributor to the etiology of primary dystonia.

LAP1 and LULL1 Have a Similar Mode of Action. The LDs of LAP1 and LULL1 are 60% identical on the level of primary structure, suggesting that they operate via a similar mechanism. If these cofactors would, however, accelerate distinct steps of the ATPase cycle (e.g., ATP hydrolysis or nucleotide dissociation), we would expect to see synergy between the two when added simultaneously. However, an equimolar mixture of LAP1 and LULL1 (each 1.5 μM) stimulates ATP hydrolysis to a level that closely matches

the arithmetic mean between the separate rates obtained for 3.0 μM LAP1 or LULL1 added individually (Fig. 3*B*); that is, a synergistic effect was not observed. This finding argues against the possibility that LAP1 and LULL1 accelerate distinct steps of the ATPase cycle.

LULL1 Is a More Potent Inducer of TorsinA ATPase Activity than LAP1. Next, we determined kinetic parameters of the ATPase reaction. We varied the concentration of LAP1 or LULL1 while leaving the TorsinA concentration constant. We observed hyperbolic saturation curves both for LAP1 and LULL1 titrations (Fig. 3 *C* and *D*). The data were fitted to Michaelis–Menten kinetics and yielded maximal velocities of 0.075 ± 0.007 μM·min^{-1} and 0.14 ± 0.005 μM·min^{-1} for LAP1 and LULL1, respectively. These values correspond to turnover numbers of 0.16 min^{-1} and 0.47 min^{-1} relative to a TorA monomer. Half-maximal stimulation was seen in presence of 1.93 μM LAP1 or 0.65 μM LULL1, respectively.

Thus, LULL1 is a more potent inducer of TorsinA ATPase activity than LAP1 for two reasons: (*i*) LULL1 has an approximately threefold-higher affinity for TorA than LAP1 (this is only an approximation based on apparent K_m values), and (*ii*) LULL1 stimulates the ATPase to an approximately threefold higher V_{max}.

We next assessed the stoichiometry of LAP1/LULL1 binding via Job plot analysis (21). To this end, we measured the ATPase activity in the presence of varying LAP1 or LULL1:TorA ratios while leaving the sum of the concentrations of TorA and cofactor constant. For LAP1, maximum intensity was observed at a ratio that is very close to 1:1 (LAP1 monomer:TorA monomer) (Fig. 3*E*). For LULL1, maximum ATPase activity was seen at a ratio of ~0.26–0.28:1 (LULL1 monomer:TorA mono-

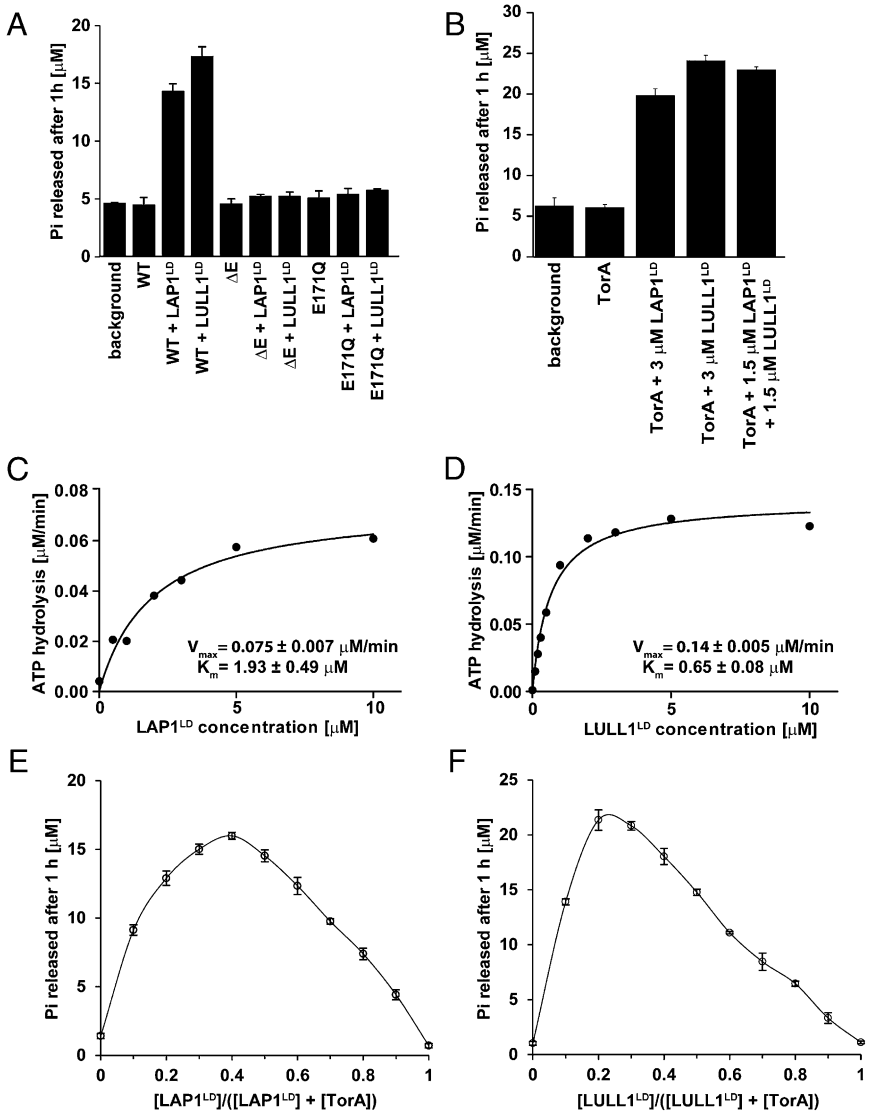

Fig. 3. LAP1 and LULL1 stimulate the ATPase activity of TorsinA. (*A*) TorsinA and its mutant derivatives were incubated in presence of 2 mM ATP, either alone or in presence of the LDs of LAP1^{LD} or LULL1^{LD}. Pi production as measure of ATP hydrolysis was monitored after 60 min using a malachite green assay. (*B*) Next, 3 μM TorA was incubated at with 3 μM LAP1^{LD} or LULL1^{LD} individually or a combination of both 1.5 μM LAP1^{LD} and 1.5 μM LULL1^{LD}. Pi release was monitored after 60 min. (*C* and *D*) Initial velocities of ATP hydrolysis were obtained after monitoring Pi release in presence of 3 μM TorsinA and increasing LAP1^{LD} (*C*) or LULL1^{LD} (*D*) concentrations as indicated. To increase the signal, the assay for LAP1^{LD} was performed in 40 μL instead of 25 μL. The data were fitted to Michaelis–Menten kinetics in Prism and yielded the indicated apparent K_m and V_{max} values. (*E* and *F*) Job plot analysis to assess the stoichiometry of LAP1^{LD}/LULL1^{LD} binding to TorA. The total concentration of LAP1^{LD} (or LULL1^{LD}) and TorA in the ATPase assay was kept constant at 10 μM while varying the ratios of individual components.

mer) (Fig. 3*F*). Thus, LULL1 and LAP1 bind to TorA with distinct stoichiometries.

Reconstitution of Torsin A in Proteoliposomes. Given that the ATPase activity of TorA is low compared with other ATPases even in the presence of LAP1 or LULL1, we tested whether lipids have a stimulatory effect on activity, as is often seen for membrane proteins. To this end, TorA was incubated with a mixture of lipids that resembles the composition of ER membranes (22, 23), either alone or in the additional presence of LAP1 or LULL1. The ATPase activity in either case was comparable to control reactions that were preformed with DDM-solubilized TorA (Fig. 4*A*).

We next reconstituted TorA in proteoliposomes to more closely mimic its physiologically relevant environment in apposition to a lipid bilayer. To assess the orientation of TorA in these proteoliposomes, we performed a protease protection assay. The majority of TorA was readily degraded upon addition of proteinase K, even in the absence of detergent, indicating that TorA preferentially adopts an outside-facing orientation on proteoliposomes (Fig. 4*B*). In this orientation, TorA is accessible to exogenously added nucleotides or cofactors. A small percentage of TorA was protease-resistant unless Nonidet P-40 was additionally added, suggesting that a minor fraction of TorA was luminal.

We then compared the ATPase activity of these proteoliposomes with free (i.e., DDM-solubilized) TorA under conditions where the total concentration of TorA in both samples is identical (Fig. 4*C*). In a direct comparison, the activity of TorA in proteoliposomes is slightly lower than for free TorA, both in the presence of LAP1 and LULL1 (Fig. 4*A*). We speculate that the somewhat lower activity is attributable to a loss of biological activity during the reconstitution process and because of the fact that a small portion of TorA is luminal, and therefore inaccessible to LAP1 and LULL1.

Taken together, these data demonstrate that the low ATPase activity of TorA cannot be attributed to the lack of lipids that would be present in a physiological setting.

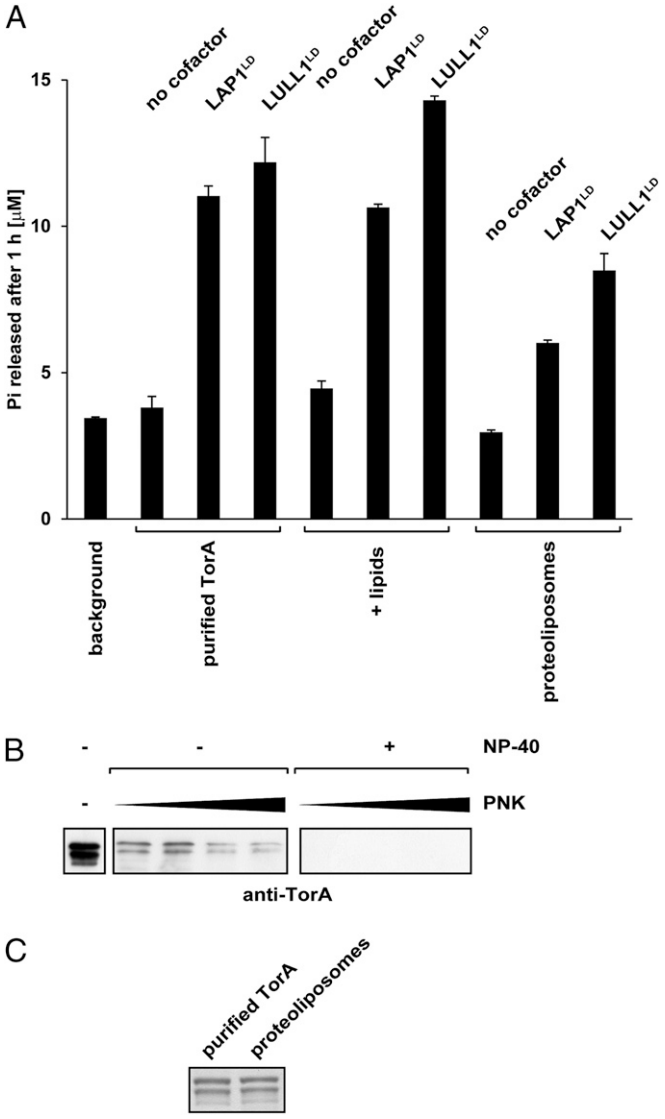

Fig. 4. Reconstitution of TorsinA in proteoliposomes. (*A*) The ATPase activity was measured for detergent-solubilized and reconstituted TorA. ER lipids (*Methods*) were added to detergent-solubilized TorA to a final concentration of 300 μM. (*B*) Proteoliposomes were incubated with increasing concentrations of proteinase K (PNK), in the absence or presence of Nonidet P-40, and subjected to SDS/PAGE and immunoblotting. (*C*) The amount of detergent-solubilized TorA and TorA in the proteoliposomes used in above ATPase assay was compared via SDS/PAGE and colloidal blue staining.

Are LAP1 and LULL1 Substrates or Cofactors? For many AAA ATPases that act to unfold substrates, the substrate itself can stimulate ATP hydrolysis. It is therefore unclear whether LAP1 and LULL1 are bona fide cofactors or merely substrates. We therefore tested whether LAP1 or LULL1 are unfolded in the presence of TorA. We set up a system that allows us to capture unfolded species using a GroEL D87K "trap" variant, which binds to unfolded species with high affinity, resulting in their sequestration into the central GroEL cavity (24). The underlying rationale is that any unfolded LAP1 or LULL1 species that would be produced by TorA's putative unfolding activity will immediately be sequestered by the GroEL trap (present in excess), which is easily separated from native species via size-exclusion chromatography (25, 26).

To validate our approach, we included positive controls in which we chemically denatured LAP1 or LULL1 using 8 M urea, followed by rapid dilution into a reaction mixture that was then chromatographically separated. Under these conditions, we can robustly detect unfolded LAP1/LULL1 species in association with the GroEL trap, as judged by a profound shift of LAP1/LULL1 to GroEL-containing fractions that were subjected to immunoblotting with anti-LAP1/anti-LULL1 antisera (Fig. 5). Thus, we would easily detect if even a small fraction of LAP1/LULL1 would be unfolded by TorA. However, we failed to detect any evidence for an unfolding activity, as judged by a complete lack of GroEL trap-associated LAP1/LULL1 species in presence of TorA and an ATP-regenerating system. We therefore consider a LAP1/LULL1-directed threading/unfolding activity for TorA unlikely. However, we cannot formally exclude that LAP1/LULL1 are substrates in an in vivo setting.

LAP1 and LULL1 Accelerate the Hydrolysis Step of the ATPase Cycle. The unfolding experiment argues against but does not exclude a possible role for LAP1/LULL1 as substrates. We therefore tested whether LAP1/LULL1 act as ATPase activators. Most commonly, GTPase or ATPase activators function by accelerating nucleotide hydrolysis or by modulating nucleotide affinity. We exploited the fact that TorA's ATPase activity is negligible in the absence of cofactors and isolated complexes of TorA and α-32P ATP via rapid (~2 min) gel filtration at 4 °C. We used the resulting complexes to perform single turnover assays in which we can simultaneously determine α-32P ADP and α-32P ATP concentrations at a time of choice after separation via TLC, providing a direct readout for the ATP hydrolysis step.

In agreement with our steady-state measurements (Fig. 3), ATP hydrolysis is negligible in the absence of cofactors (Fig. 6*A*). We then added either cofactor to a final concentration of 10 μM

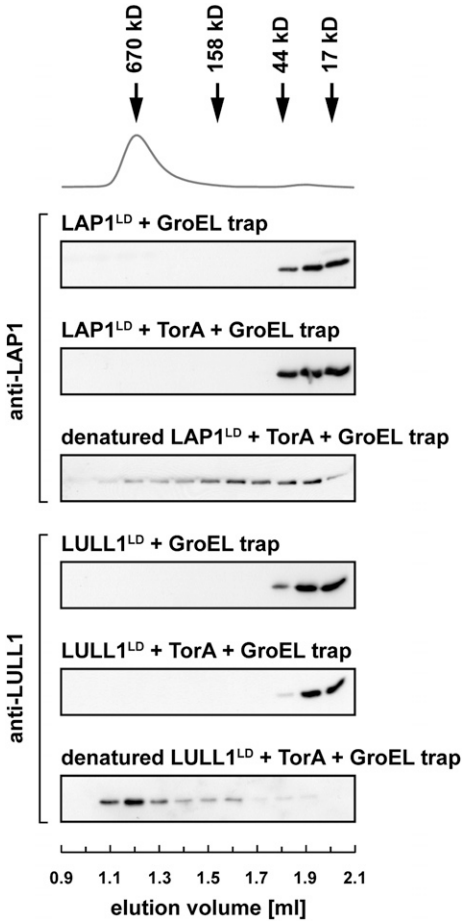

Fig. 5. LAP1 and LULL1 are not unfolded by TorsinA. Native LAP1^{LD} or LULL1^{LD} were incubated in presence of GroEL D87K and an ATP-regenerating system, or in the additional presence of TorA. After 30 min, the reaction mixtures were applied onto a Superdex 200 PC column and eluted with trap buffer. Fractions were collected and separated by SDS/PAGE, and subjected to immunoblotting using antisera against LAP1 or LULL1. The UV elution profile of GroEL D87K and the positions of size markers are included for reference. As positive control, LAP1^{LD} or LULL1^{LD} were denatured in 8 M urea, and rapidly diluted 1:50 into otherwise identical reactions.

that was found to be saturating under steady-state conditions (Fig. 3 *C* and *D*). ATP hydrolysis is rapidly induced upon addition of LAP1 and, consistent with our observations under steady-state conditions, more potently upon addition of LULL1 (Fig. 6*A*).

The fact that TorsinA and TorsinB are 68% identical in primary structure, as well as functionally redundant in murine cells (5), prompted us to investigate whether TorsinB is similarly activated by LAP1 or LULL1. This was indeed the case (Fig. 6*B*). The resulting rate constants (Fig. 6*C*) inform us that for both TorA and TorB, the ATP hydrolysis step is strongly accelerated by either cofactor, up to almost two orders of magnitude in the case of TorB/LULL1 (Fig. 6*D*).

This is strong evidence that it is specifically the hydrolysis step that is tightly regulated by LAP1 and LULL1. The observed magnitude of stimulation provides a gratifying mechanistic explanation for our data obtained under steady-state conditions, specifically (*i*) the negligible activity in absence of cofactors (Fig. 3*A*) and (*ii*) the lack of synergy between LAP1 and LULL1 (Fig. 3*B*). To our knowledge, this report of an AAA+ ATPase whose hydrolysis step is subject to tight regulation via bona fide ATPase activators is unique.

Distinct Regulation of Torsins by Their Cofactors. We next investigated whether the remaining representatives of the Torsin family are similarly regulated. We purified Torsin2A and Torsin3A and measured their ATPase activities. Either ATPase alone was essentially inactive (Fig. 7), as previously observed for Torsin A and B (Figs. 3*A* and 6 *A* and *B*). Surprisingly, Tor2A was not significantly stimulated upon addition of either LAP1

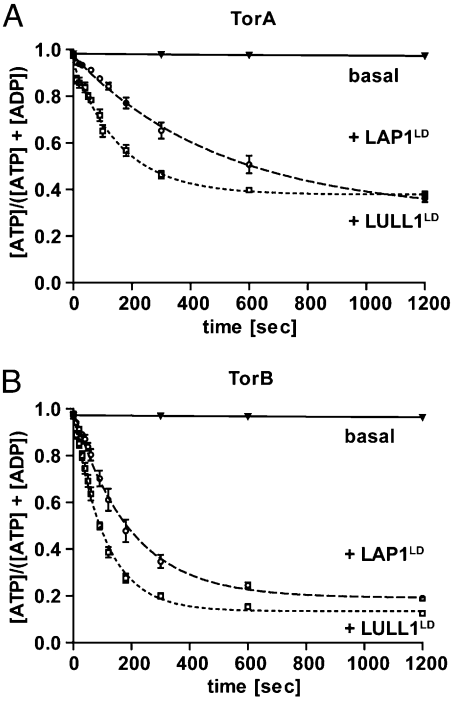

C rate constants [min^{-1}]

	basal	+ LAP1^{LD}	+ LULL1^{LD}
TorA	0.01 ± 0.006	0.12 ± 0.01	0.37 ± 0.04
TorB	0.006 ± 0.001	0.31 ± 0.02	0.55 ± 0.02

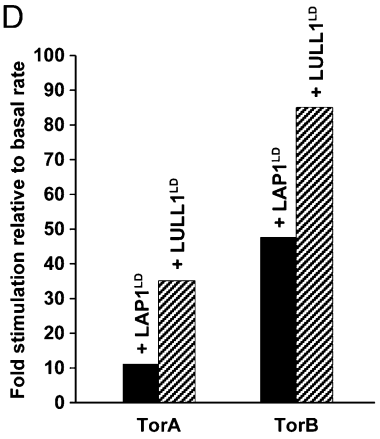

Fig. 6. LAP1^{LD} and LULL1^{LD} specifically accelerate the ATP hydrolysis step of the ATPase cycle. (*A* and *B*) Single turnover kinetics of TorA/B ATPases alone (basal rate) or in presence of the indicated cofactor. Data represent a mean obtained from three independent experiments. Error bars indicate the SD. (*C*) Rate constants obtained from fitting the data above to a single exponential decay function, using Prism. (*D*) Stimulation of TorA/B by LAP1^{LD}/LULL1^{LD} relative to the basal rate as observed in *A* and *B*.

or LULL1, whereas Tor3A was only stimulated by LULL1 but not by LAP1 (Fig. 7).

Thus, the LAP1/LULL1-mediated activation mechanism that we identified for TorA is conserved for TorB, with the latter being the more potent ATPase (Figs. 6*C* and 7). Surprisingly, Tor2A does not effectively respond to either cofactor, and Tor3A is only activated by LULL1.

Discussion

How the activity of Torsin ATPases is regulated is currently unknown. LAP1 and LULL1 are NE components that are found in association with TorA (16, 20). Overexpression of these factors profoundly changed the subcellular localization of TorA or specific mutant derivatives, suggesting an important role for these cofactors (9, 16). Furthermore, a LAP1-deficient mouse model phenocopies certain features of TorA-deficient animals (5). Taken together, these observations prompted us to investigate the mechanistic relationship between LAP1, LULL1, and TorsinA.

We showed that TorA physically associates with LAP1 and LULL1. This interaction is direct (Fig. 2) and is mediated by the LDs of these related type II transmembrane proteins (Figs. 1 *E* and *F*, and 2). Only TorA E171Q, a hydrolysis-deficient trap mutant of TorA, binds to LAP1 and LULL1 with high affinity, as judged by coimmunoprecipitation experiments (Fig. 1 *A* and *B*), and does so in nucleotide-dependent fashion (Fig. 2 *C* and *D*). This interaction is interrupted by the DYT1 dystonia-causing mutation, ΔE (Figs. 1 *A* and *B*, and 2*E*), again suggesting a functionally relevant relationship between LAP1/LULL1 and TorsinA.

What are the functions of LAP1 and LULL1? Having demonstrated that the LDs are necessary and sufficient for TorA binding (Fig. 1 *E* and *F*), we purified these domains along with full-length TorA and asked whether their presence or absence has an impact on the ATPase activity of TorsinA. We found that TorA alone is essentially inactive (Figs. 3*A* and 6*A*). However, ATPase activity was induced in the presence of LAP1 or LULL1, and activity increased with addition of LAP1 and LULL1 in a dose-dependent fashion. LULL1 was significantly more efficient at accelerating ATPase activity than LAP1, as judged by an approximately threefold lower apparent K_m and approximately threefold higher V_{max}, respectively (Fig. 3 *C* and *D*). Strikingly, TorA ΔE failed to respond to either LAP1 or LULL1, even at concentrations that are saturating for TorA WT (Fig. 3*A*).

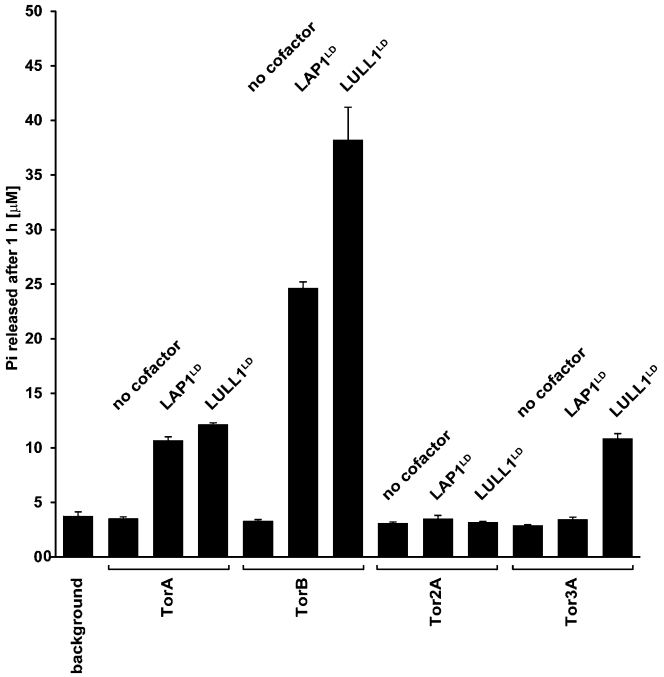

Fig. 7. Regulation of the Torsin family by LAP1 and LULL1. Three micromolars of each Torsin was incubated in presence of 2 mM ATP, either alone or in presence of the LDs of LAP1 or LULL1. Pi production as measure of ATP hydrolysis was monitored after 60 min using a malachite green assay.

Taking into account our single turnover measurements (Fig. 6), our observations are consistent with a model where LAP1 or LULL1 bind to TorA in the ATP-bound state to trigger ATP hydrolysis. Although our data do not rule out a possible role as substrates, we strongly favor a regulatory function for the following reasons: First, LULL1 and LAP1 affect the subcellular localization of specific TorA variants, whereas TorA did not have an impact on LULL1 or LAP1 localization (9, 16). Second, TorA did not display a LAP1/LULL1-directed unfolding activity (Fig. 5). Apart from activating Torsin ATPases, LAP1 or LULL1 may additionally serve as substrate adaptors, although this additional role is at present purely speculative. It will be interesting to study how the differential stimulation of Torsins by their cofactors (Fig. 7) correlates with biological activity, and to determine how the binding of cofactors is relayed to the ATPase active site. The fact that Tor2A associates with LAP1 (5) despite being unresponsive to its stimulation (Fig. 7) suggests a rather complex mechanistic relationship for these interactions, the structural underpinnings and biological relevance of which remain to be established.

It is noteworthy that the ATPase activity of all Torsins is comparatively low even in the presence of saturating cofactor concentrations (Figs. 3, 6*D*, and 7). This finding we attribute to the presence of a noncanonical Walker A motif that is conserved among all Torsins (i.e., GxxxxGKN rather then GxxxxGKS/T). Indeed, a Thr to Asn mutation in the Walker A motif of the homologous AAA ATPase ClpB (to mimic the Walker A motif of TorA) substantially reduces its ATPase activity (27). Nevertheless, it will be interesting to test whether substrates additionally stimulate the activity of their cognate Torsin ATPases. α-Casein, a constitutively misfolded protein that stimulates a host of AAA+ ATPases implicated in protein quality control, including other membrane-associated representatives (28, 29), did not stimulate the activity of TorA (Fig. S4). This property, as well as the noncanonical Walker A motif, sets Torsins apart from the majority of AAA+ ATPases that possess an unfoldase function that is directed to misfolded proteins.

Our study provides a mechanistic rationale for many phenotypic observations that were made in the context of animal models. First, the fact that similar phenotypes were observed in LAP1- and TorA-deficient mice had previously suggested that LAP1- and TorA act in one pathway (5): we propose that because of the lack of LAP1, the TorA ATPase activity is essentially kept off in the NE. Second, our findings explain why LAP1 deficiency results in a stronger phenotype than TorA deficiency (5): LAP1 is required both for TorA and TorB activation (Fig. 6*B*). We suggest that TorB can partially compensate for the missing TorA function in nonneuronal tissues in Tor1A$^{-/-}$ or Tor1A$^{\Delta gag/\Delta gag}$ animals, whereas a LAP1 knockout will essentially be equivalent to a TorA/TorB double-knockout. It will be interesting to test this prediction experimentally. Third, our data demonstrate a loss-of-function mechanism for the TorA ΔE dystonia mutation, thus explaining why a Tor1A$^{\Delta gag/\Delta gag}$ "knock-in" in mouse model fails to rescue the Tor1A$^{-/-}$ phenotype (6).

How the formation of NE vesicles seen as part of the Tor1A$^{-/-}$ or Lap1$^{-/-}$ phenotype is related to the TorA ATPase remains to be established. NE dynamics are not limited to cell division, but they also occur in interphase cells. Examples include the occurrence of intraluminal vesicles in neurons (30) or during viral infection (31, 32), and NE invaginations that reach into the nucleoplasm (33). Given that AAA+ ATPases, such as NSF and VPS4, are

implicated in various forms of membrane dynamics (3, 34, 35), one may speculate that NE-resident Torsin ATPases are prime candidates to be relevant for membrane dynamics of the NE (31, 36). So far no NE abnormalities have been observed upon LULL1 manipulation (5, 9), suggesting that LAP1 is primarily important for TorA function in the NE. Apparently, LULL1 and LAP1 are not functionally redundant.

Whether TorA has a direct role in the formation of vesicular structures (30, 31, 36) or whether their appearance is merely an indirect consequence of TorA inactivation is at present unknown. We believe that the many distinct functions that have been proposed for TorA (ref. 4 and references cited therein) depend on the association of specific cofactors that serve both to recruit this ATPase to specific cellular sites and to activate its ATPase activity. Given that TorA associates with components of the NE-resident LINC (linker of nucleoskeleton and cytoskeleton) complex and changes their localization (9, 37), it will be interesting to test whether TorA plays a role in assembly or disassembly of these NE bridges. Having established a robust in vitro system for studying TorsinA and its regulatory cofactors, this work provides the basis to further scrutinize TorsinA functions from a mechanistic perspective and deepens our understanding of molecular defects underlying DYT1 dystonia.

Methods

Constructs for Mammalian Cell Expression, Cell Lines, and Transient Transfections. All constructs were cloned into pcDNA3.1$^+$ vector using PCR-based standard procedures. Full-length LAP1 and LULL1 constructs were cloned with an N-terminal FLAG tag. LAP1 and LULL1 LDs (LAP1^{LD} or LAP1$^{356\text{-}583}$, and LULL1^{LD} or LULL1$^{236\text{-}470}$) were cloned with an N-terminal MHC-I HLA-A signal sequence and a C-terminal HA tag. LAP1 cytosolic/nuclear domain (LAP1$^{1–339}$) and LULL1 cytosolic/nuclear domain (LULL1$^{1–215}$) were cloned with an N-terminal HA tag and a C-terminal farnesylation sequence from Lamin B1 (ASNRS-CAIM) (LAP1$^{CND\text{-}F}$ and LULL1$^{CND\text{-}F}$). HEK293T and HeLa cells were grown in a humidified atmosphere and 5% (vol/vol) CO_2 in DMEM supplemented with 10% (vol/vol) FBS. HEK293T cells were transfected at ~80% confluence using Lipofectamine 2000 (Invitrogen), and HeLa cells were transfected using X-tremeGENE DNA (Roche). Experiments were performed 24 h posttransfection unless otherwise specified.

Metabolic Labeling, Immunoprecipitation, and Immunoblotting. Twenty-four hours posttransfection, HEK293T cells were metabolically labeled with 800 μCi of [^{35}S] methionine/cysteine (PerkinElmer) at 37 °C overnight. The cells were washed twice with ice-cold PBS and lysed with lysis buffer (50 mM Tris, pH 7.5, 75 mM NaCl, 5 mM $MgCl_2$, and 0.5% Nonidet P-40) supplemented with 2 mM ATP and complete (Roche) protease inhibitors on ice for 10 min. After centrifugation (20,000 × *g*, 4 °C, 10 min), supernatants were precleared with Protein A agarose (RepliGen) for 1 h followed by immunoprecipitation with HA affinity beads (Roche) at 4 °C for 3 h. Beads were washed with lysis buffer four times, boiled in SDS loading buffer, and subjected to SDS/PAGE. Immunoblotting was performed according to standard procedures, using the Western Lightning *Plus* ECL chemiluminescence kit (PerkinElmer) and X-ray films (Kodak) for detection.

Cloning, Bacterial Expression, and Purification of LAP1^{LD} and LULL1^{LD}. The luminal segments of LAP1 (LAP1^{LD} or LAP1$^{356–583}$) and LULL1 (LULL1^{LD} or LAP1$^{236–470}$) were cloned via PCR into a modified pET28b vector containing a PreScission Protease restriction site between a His-tag and the fused protein. LULL1^{LD} was expressed in Origami 2(DE3)pLysS cells (Novagen). The cells were grown at 30 °C in DYT medium [1.6% (wt/vol) tryptone, 1% yeast extract, and 0.5% NaCl, pH 7.0) supplemented with 50 μg/mL kanamycin and 34 μg/mL Chloramphenicol to OD_{600} of 1.0 and protein production was induced with 1 mM isopropyl-β-D-thiogalactopyranoside at 18 °C overnight. The cells were harvested by centrifugation at 6,000 × *g* for 15 min and the pellet was resuspended in binding buffer (20 mM sodium phosphate, 0.5 M NaCl, 10 mM imidazole, pH 7.4) supplemented with Complete (Roche) protease inhibitors (Roche). Cells were disrupted using a microfluidizer at a pressure of 15,000 psi. After removal of the insoluble fraction by centrifugation at 26,000 × *g* for 40 min, the supernatant was incubated with 1 mL Ni Sepharose 6 Fast Flow resin (GE Lifesciences) at 4 °C for 1 h. Unbound material was removed with 30 mL binding buffer. His-tagged LULL1^{LD} was eluted with 5 mL elution buffer (20 mM sodium phosphate, 0.5 M NaCl, 500 mM imidazole, pH 7.4). The eluate was immediately diluted 10-fold with ion exchange binding buffer (25 mM Tris and 50 mM NaCl, pH 7.5) and applied to a Resource Q column (GE Lifesciences). The protein was eluted with a linear gradient to 1 M NaCl in 20 column volumes, pooled and incubated with PreScission protease (GE Lifesciences) (20 units/mg LULL1^{LD}) overnight to remove the His-tag. PreScission protease was removed by gel filtration using a Superdex 75 HiLoad column (GE Lifesciences). For snap-freezing in liquid nitrogen, 10% (vol/vol) glycerol was added to the protein solution.

LAP1^{LD} was expressed in Rosetta(DE3)pLysS cells (Novagen) at 30 °C and purified as described for LULL1, except that the ion-exchange step was omitted.

Antibodies. Anti-FLAG antibody was purchased from Sigma-Aldrich and anti-HA antibody (3F10) was purchased from Roche. Antibodies against LaminA and LaminB1 were purchased from Abcam. Goat anti-rabbit, anti-mouse, and anti-rat conjugated to Alexa Flour dyes were purchased from Invitrogen. Goat anti-rabbit and anti-mouse IgG HRP conjugated antibodies were purchased from Thermo Scientific. A TorA fragment lacking the N-terminal signal sequence and hydrophobic segment was expressed in Rosseta(DE3) pLysS cells (Novagen) and purified via His-tag for antiserum production (Covance). The anti-LAP1 and anti-LULL1 antisera were raised against the above purified LAP1^{LD} and LULL1^{LD} (Covance).

Cloning, Expression, and Purification of Human Torsins. Human Torsins and its mutant derivatives were PCR-amplified to install a C-terminal His10-tag followed by a Flag-tag and cloned into pFastBac I vector (Invitrogen). The recombinant baculovirus generation and amplification were performed as described by Invitrogen. Torsins were expressed for 72 h in Sf9 cells infected with the recombinant baculovirus at a multiplicity of infection of 2. For purification, the cells were centrifuged at 1,000 × *g* and 4 °C for 10 min and the pellet was washed with ice-cold PBS (pH 7.4). The cells were solubilized with lysis buffer [20 mM Hepes, 150 mM NaCl, 5 mM $MgCl_2$, 5 mM KCl, 10% (vol/vol) glycerol, and 1% (wt/vol) DDM, pH 8.0] supplemented with Complete (Roche) protease inhibitors at 4 °C for 1 h and centrifuged at 20,000 × *g* for 30 min. The supernatant was incubated with 1 mL Anti-FLAG M2 Affinity Gel (Sigma) equilibrated with equilibration buffer (20 mM Hepes, 150 mM NaCl, 5 mM $MgCl_2$, 5 mM KCl, 10% glycerol, and 0.05% DDM, pH 8.0) at 4 °C for 3 h followed by washing with 20 column volumes of equilibration buffer. TorA was eluted by incubating with 5 column volumes of 300 μg/mL FLAG peptide in equilibration buffer at 4 °C for 1 h. The eluate was subjected to 0.5 mL of His-Select Nickel Affinity Gel (Sigma) at 4 °C for 3 h in the presence of 10 mM imidazole. After washing with 20 column volumes of equilibration buffer (20 mM Hepes, 150 mM NaCl, 5 mM $MgCl_2$, 5 mM KCl, 10% (vol/vol) glycerol, and 0.05% DDM, pH 8.0) supplemented with 10 mM imidazole, Torsins were eluted with 5 column volumes of 150 mM imidazole in equilibration buffer. Imidazole was removed by PD-10 column from GE Healthcare. For long-term storage, Torsins were snap-frozen in liquid nitrogen and stored at –80 °C.

ATPase Activity Assay. For ATPase activity assay, 3 μM of purified TorA was incubated in 25 μL equilibration buffer (20 mM Hepes, 150 mM NaCl, 5 mM $MgCl_2$, 5 mM KCl, 10% glycerol, and 0.05% DDM, pH 8.0) supplemented with 2 mM ATP at 37 °C for 1 h, in the presence or absence of LAP1^{LD} or LULL1^{LD}. The reaction was terminated with 175 μL of 20 mM sulfuric acid (H_2SO_4). The concentration of inorganic phosphate (Pi) was determined by a colorimetric method (38). Fifteen minutes after the addition of 50 μL of freshly prepared malachite green solution [0.096% malachite green, 1.48% (wt/vol) ammonium molybdate, and 0.173% Tween-20 in 2.9 M H_2SO_4], the absorbance was measured at 620 nm in a 96-well plate reader (BioTek). Measurements were performed in triplicate under conditions giving a linear rate of product formation (Pi). Calibration of free phosphate concentration was carried out with Na_2HPO_4 in 200 μL of 20 mM H_2SO_4. Data analysis was performed in Prism.

For single turnover assays, 50 μM Torsin was incubated with 100 μCi of α-32P (800 Ci/mmol; Perkin-Elmer) ATP for 3 min at 30 °C in a total volume of 100 μL and chilled on ice. Free ATP was separated from TorA-bound ATP by a rapid gel filtration using a PD10 column (GE Healthcare) preequilibrated in ice-cold running buffer (30 mM Hepes, 75 mM NaCl, 5 mM $MgCl_2$, pH 7.5). Complexes were detected in the eluate using a Geiger counter, pooled, aliquoted on ice, and flash-frozen in liquid nitrogen. Single turnover assays were performed at 30 °C. Two-microliter aliquots were removed at indicated time points and resolved by TLC using PEI-Cellulose (Merck) and 400 mM LiCl in 10% (vol/vol) acetic acid as mobile phase. TLC plates were imaged using an imaging plate (GE Healthcare) and quantified densiometrically using ImageQuant. The resulting data were fitted to a single exponential decay function in Prism.

Analytical Gel Filtration. Purified TorA or mutant derivatives (5 μM) were incubated with $Lap1^{LD}$ or $LULL1^{LD}$ (10 μM) in gel-filtration buffer [25 mM Tris, 75 mM NaCl, 5 mM $MgCl_2$, 5 mM KCl, 5% (vol/vol) glycerol, and 0.05% (wt/vol) DDM, pH 7.5], in the presence or absence of 2 mM ATP at 30 °C for 5 min and subjected to a Superdex 200 PC 3.2/30 column on a Purifier system (GE Healthcare). The protein was eluted with gel-filtration buffer in the presence or absence of 0.5 mM ATP, at a flow rate of 50 μL/min. The absorbances at 280 nm were recorded. Fractions of 100 μL were collected and analyzed by SDS/PAGE (12%) and immunoblotting. Soluble protein standards from Bio-Rad were used for column calibration.

Proteoliposome Reconstitution. Reconstitution of TorA was performed as described previously (39). In short, ER membrane lipids were prepared by mixing cholesterol and phospholipids [55%(mol/mol) dioleoylphosphatidylcholine (DOPC), 20% dioleoylphosphatidylethanolamine (DOPE), 5% dioleoylphosphatidylserine (DOPS), 5% dioleoylphosphatidic acid (DOPA), and 15% phosphatidylinositol (PI)] in a molar ratio of 0.15. After removing the organic solvent, the lipids were rehydrated in reconstitution buffer (30 mM Hepes, 100 mM NaCl, 5 mM $MgCl_2$, pH 7.5). To prepare large unilaminar vesicles, the liposomes were snap-frozen in liquid N_2 and thawed at room temperature for five cycles followed by extrusion through a 400-nm polycarbonate filter (Avestin). The large unilaminar vesicles were diluted to 2.5 mg/mL and destabilized by 10% (wt/vol) Triton X-100, and followed by incubation with TorA with a molar ratio of 700:1 (lipids to TorA) at 4 °C for 30 min. After removal of detergents by addition of Bio-beads (Bio-Rad), the proteoliposomes were sedimented by centrifugation (300,000 × *g* for 45 min) and resuspended in 450 μL reconstitution buffer.

GroEL Trap Assay. GroEL D87K (GroEL "trap," plasmid kindly provided by Art Horwich, Yale School of Medicine, New Haven, CT and Howard Hughes Medical Institute) was purified as described previously (40). $Lap1^{LD}$ or $Lull1^{LD}$ was diluted to 0.3 μM in trap buffer (25 mM Tris, 150 mM NaCl, 5 mM $MgCl_2$, 5 mM KCl, pH 7.5) containing 7 μM GroEL D87K, 2 mM ATP, 3 mM phosphoenolpyruvate and 1 U pyruvate kinase (PK) at 30 °C for 30 min, in the presence or absence of 0.3 μM TorA. As a control, 8 M urea was incubated with 50-fold $LAP1^{LD}$ or $LULL1^{LD}$ before a 1:50 dilution to a final concentration of 300 nM in the unfolding reaction. The reaction mixture was applied onto a Superdex 200 PC column and eluted with trap buffer.

ACKNOWLEDGMENTS. We thank members of the C.S. laboratory for comments on the manuscript and Art Horwich for providing the GroEL D87K plasmid. This work was funded by the Ellison Medical Foundation (AG-NS-0662-10) and National Institutes of Health (DP2 OD008624-01).

1. Ozelius LJ, et al. (1997) The early-onset torsion dystonia gene (DYT1) encodes an ATP-binding protein. *Nat Genet* 17(1):40–48.
2. Neuwald AF, Aravind L, Spouge JL, Koonin EV (1999) AAA+: A class of chaperone-like ATPases associated with the assembly, operation, and disassembly of protein complexes. *Genome Res* 9(1):27–43.
3. Hanson PI, Whiteheart SW (2005) AAA+ proteins: Have engine, will work. *Nat Rev Mol Cell Biol* 6(7):519–529.
4. Atai NA, Ryan SD, Kothary R, Breakefield XO, Nery FC (2012) Untethering the nuclear envelope and cytoskeleton: biologically distinct dystonias arising from a common cellular dysfunction. *Int J Cell Biol* 2012:634214.
5. Kim CE, Perez A, Perkins G, Ellisman MH, Dauer WT (2010) A molecular mechanism underlying the neural-specific defect in torsinA mutant mice. *Proc Natl Acad Sci USA* 107(21):9861–9866.
6. Goodchild RE, Kim CE, Dauer WT (2005) Loss of the dystonia-associated protein torsinA selectively disrupts the neuronal nuclear envelope. *Neuron* 48(6):923–932.
7. Hewett J, et al. (2000) Mutant torsinA, responsible for early-onset torsion dystonia, forms membrane inclusions in cultured neural cells. *Hum Mol Genet* 9(9):1403–1413.
8. Callan AC, Bunning S, Jones OT, High S, Swanton E (2007) Biosynthesis of the dystonia-associated AAA+ ATPase torsinA at the endoplasmic reticulum. *Biochem J* 401(2): 607–612.
9. Vander Heyden AB, Naismith TV, Snapp EL, Hodzic D, Hanson PI (2009) LULL1 retargets TorsinA to the nuclear envelope revealing an activity that is impaired by the DYT1 dystonia mutation. *Mol Biol Cell* 20(11):2661–2672.
10. Liu Z, Zolkiewska A, Zolkiewski M (2003) Characterization of human torsinA and its dystonia-associated mutant form. *Biochem J* 374(Pt 1):117–122.
11. Vander Heyden AB, Naismith TV, Snapp EL, Hanson PI (2011) Static retention of the lumenal monotopic membrane protein torsinA in the endoplasmic reticulum. *EMBO J* 30(16):3217–3231.
12. Gonzalez-Alegre P, Paulson HL (2004) Aberrant cellular behavior of mutant torsinA implicates nuclear envelope dysfunction in DYT1 dystonia. *J Neurosci* 24(11):2593–2601.
13. Goodchild RE, Dauer WT (2004) Mislocalization to the nuclear envelope: An effect of the dystonia-causing torsinA mutation. *Proc Natl Acad Sci USA* 101(3):847–852.
14. Naismith TV, Heuser JE, Breakefield XO, Hanson PI (2004) TorsinA in the nuclear envelope. *Proc Natl Acad Sci USA* 101(20):7612–7617.
15. Foisner R, Gerace L (1993) Integral membrane proteins of the nuclear envelope interact with lamins and chromosomes, and binding is modulated by mitotic phosphorylation. *Cell* 73(7):1267–1279.
16. Goodchild RE, Dauer WT (2005) The AAA+ protein torsinA interacts with a conserved domain present in LAP1 and a novel ER protein. *J Cell Biol* 168(6):855–862.
17. Schirmer EC, Florens L, Guan T, Yates JR, 3rd, Gerace L (2003) Nuclear membrane proteins with potential disease links found by subtractive proteomics. *Science* 301(5638): 1380–1382.
18. Hetzer MW, Wente SR (2009) Border control at the nucleus: Biogenesis and organization of the nuclear membrane and pore complexes. *Dev Cell* 17(5):606–616.
19. Zhang X, et al. (2000) Structure of the AAA ATPase p97. *Mol Cell* 6(6):1473–1484.
20. Naismith TV, Dalal S, Hanson PI (2009) Interaction of torsinA with its major binding partners is impaired by the dystonia-associated DeltaGAG deletion. *J Biol Chem* 284(41): 27866–27874.
21. Cantor, CR, Schimmel PR (1980) *Biophysical Chemistry: Part III* (W. H. Freeman, San Francisco), pp 1135–1139.
22. van Meer G, Voelker DR, Feigenson GW (2008) Membrane lipids: Where they are and how they behave. *Nat Rev Mol Cell Biol* 9(2):112–124.
23. Davison SC, Wills ED (1974) Studies on the lipid composition of the rat liver endoplasmic reticulum after induction with phenobarbitone and 20-methylcholanthrene. *Biochem J* 140(3):461–468.
24. Weissman JS, Kashi Y, Fenton WA, Horwich AL (1994) GroEL-mediated protein folding proceeds by multiple rounds of binding and release of nonnative forms. *Cell* 78(4): 693–702.
25. Weber-Ban EU, Reid BG, Miranker AD, Horwich AL (1999) Global unfolding of a substrate protein by the Hsp100 chaperone ClpA. *Nature* 401(6748):90–93.
26. Schlieker C, Tews I, Bukau B, Mogk A (2004) Solubilization of aggregated proteins by ClpB/DnaK relies on the continuous extraction of unfolded polypeptides. *FEBS Lett* 578(3):351–356.
27. Nagy M, Wu HC, Liu Z, Kedzierska-Mieszkowska S, Zolkiewski M (2009) Walker-A threonine couples nucleotide occupancy with the chaperone activity of the AAA+ ATPase ClpB. *Protein Sci* 18(2):287–293.
28. Roudiak SG, Shrader TE (1998) Functional role of the N-terminal region of the Lon protease from Mycobacterium smegmatis. *Biochemistry* 37(32):11255–11263.
29. Asahara Y, et al. (2000) FtsH recognizes proteins with unfolded structure and hydrolyzes the carboxyl side of hydrophobic residues. *J Biochem* 127(5):931–937.
30. Speese SD, et al. (2012) Nuclear envelope budding enables large ribonucleoprotein particle export during synaptic Wnt signaling. *Cell* 149(4):832–846.
31. Rose A, Schlieker C (2012) Alternative nuclear transport for cellular protein quality control. *Trends Cell Biol* 22(10):509–514.
32. Johnson DC, Baines JD (2011) Herpesviruses remodel host membranes for virus egress. *Nat Rev Microbiol* 9(5):382–394.
33. Malhas A, Goulbourne C, Vaux DJ (2011) The nucleoplasmic reticulum: Form and function. *Trends Cell Biol* 21(6):362–373.
34. Hurley JH, Hanson PI (2010) Membrane budding and scission by the ESCRT machinery: It's all in the neck. *Nat Rev Mol Cell Biol* 11(8):556–566.
35. Henne WM, Buchkovich NJ, Emr SD (2011) The ESCRT pathway. *Dev Cell* 21(1):77–91.
36. Burns LT, Wente SR (2012) Trafficking to uncharted territory of the nuclear envelope. *Curr Opin Cell Biol* 24(3):341–349.
37. Nery FC, et al. (2008) TorsinA binds the KASH domain of nesprins and participates in linkage between nuclear envelope and cytoskeleton. *J Cell Sci* 121(Pt 20):3476–3486.
38. Baykov AA, Evtushenko OA, Avaeva SM (1988) A malachite green procedure for orthophosphate determination and its use in alkaline phosphatase-based enzyme immunoassay. *Anal Biochem* 171(2):266–270.
39. Zhao C, Haase W, Tampé R, Abele R (2008) Peptide specificity and lipid activation of the lysosomal transport complex ABCB9 (TAPL). *J Biol Chem* 283(25):17083–17091.
40. Quaite-Randall E, Joachimiak A (2000) Purification of GroEL from an overproducing *E. coli* strain. *Methods Mol Biol* 140:29–39.